

COMPARISON OF SYSTEM IDENTIFICATION TECHNIQUES FOR A SPHERICAL AIR-BEARING SPACECRAFT SIMULATOR

Jana L. Schwartz[†] and Christopher D. Hall[‡]

Virginia Tech has developed a testbed comprised of two independent spherical air-bearing platforms for formation flying attitude control simulation, the Distributed Spacecraft Attitude Control System Simulator. The DSACSS is intended to support a wide range of functions; as such, requiring that all controllers be robust to approximations of the system parameters is impractical. We document the process to determine an appropriate system identification technique for an air-bearing spacecraft simulator. We present an overview of many of the available techniques but focus on adaptations to classical sequential filters. We document both accuracy and computation time and conclude that further analysis of each filter type is necessary.

INTRODUCTION

In this paper, we document the process to determine an appropriate system identification technique for an air-bearing spacecraft simulator. Previous efforts have relied only on batch techniques. We begin with an introduction of Virginia Tech's Distributed Spacecraft Attitude Control System Simulator (DSACSS) and its functionality. We present the equations of motion for this system and demonstrate their dependence on the parameters. We document the process to obtain an initial estimate for the parameters from a computer model and describe the batch techniques used to refine these estimates.

The focus of this paper is a discussion of several sequential filters adapted to provides estimates of both the states and the parameters. We develop the equations for these filters, describe the software used to evaluate them, and compare the results in terms of both accuracy and computation time. For the purposes of this study we use a simplified set of equations. We conclude that further evaluation of each of the filters is necessary.

HARDWARE

Virginia Tech has developed a Distributed Spacecraft Attitude Control System Simulator (DSACSS), which includes two independent spherical air-bearing platforms for formation flying attitude control simulation. Both systems are Space Electronics, Incorporated, models: the smaller is a tabletop-style bearing that can support a 300 lb payload, shown in the foreground of Figure 1. This system, Whorl-I, can tilt $\pm 5^\circ$ from the horizontal and spin freely about the vertical (yaw) axis. Whorl-II

[†]National Science Foundation Fellow, NASA Graduate Student Researcher Program Fellow. Department of Aerospace & Ocean Engineering, Virginia Polytechnic Institute & State University, Blacksburg, Virginia 24061. jana@vt.edu. Student Member AIAA, Student Member AAS.

[‡]Professor. Department of Aerospace & Ocean Engineering, Virginia Polytechnic Institute & State University, Blacksburg, Virginia 24061. cdhall@vt.edu. Associate Fellow AIAA, Member AAS.
Copyright ©2003 by the authors. Permission to publish granted to The American Astronautical Society.

is a dumbbell-style bearing (in the background of Figure 1) that can support a 375 lb payload. It provides full freedom in both roll (about the longitudinal shaft axis) and yaw, with $\pm 30^\circ$ of freedom about the pitch axis. Each air bearing is equipped with three-axis accelerometers and rate gyros for attitude determination. Attitude control options include three-axis momentum/reaction wheels, compressed air thrusters, and control moment gyros (CMGs). The payload's center of gravity is maintained at the bearing's center of rotation via a triad of linear actuators; alternatively, attitude control schemes by center of gravity placement can be investigated.

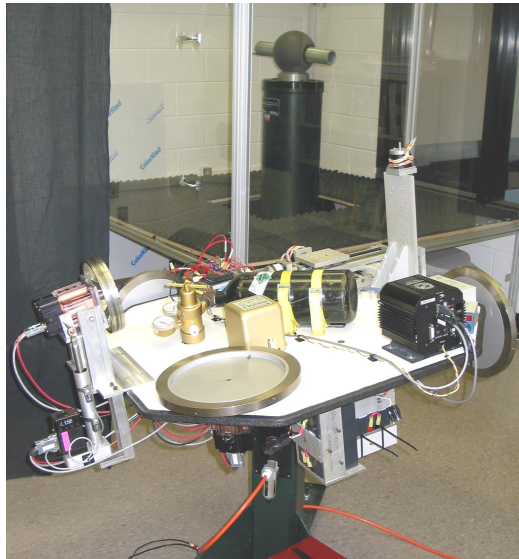


Figure 1: Virginia Tech's Distributed Spacecraft Attitude Control System Simulator

The uniqueness of this system stems not from particular individual capabilities of either platform, but rather the ability to implement distributed control laws between the two. Coupled with a third, stationary system, the DSACSS provides an experimental facility for formation flying attitude control simulation. In contrast, planar test facilities provide a motion base for testing control schemes involving the relative position and relative motion between two bodies, but coordination in pointing is difficult to replicate. The DSACSS testbed allows implementation of algorithms for relative attitude control.¹ Either of the two DSACSS air bearings can also be used independently for specialized investigations of topics in the field of spacecraft attitude dynamics and control.

EQUATIONS OF MOTION

Accurate system identification of both the state vector of attitude quaternions and body angular velocities, along with the nine-term parameter vector

$$\boldsymbol{\Pi} = \{I_{11}, I_{12}, I_{13}, I_{22}, I_{23}, I_{33}, mg\ r_{g1}, mg\ r_{g2}, mg\ r_{g3}\}^T \quad (1)$$

is crucial for successful operation of the DSACSS. We model the system with respect to the reference frame of an inertial laboratory as

$$\dot{\mathbf{q}} = \mathbf{Q}(\mathbf{q}) \boldsymbol{\omega} \quad (2a)$$

$$\dot{\boldsymbol{\omega}} = \mathbf{I}_b^{-1} \left(-\boldsymbol{\omega}^\times \mathbf{I}_b \boldsymbol{\omega} + \mathbf{g}_{wheels} + \mathbf{r}_{thruster_j}^\times \mathbf{F}_{thruster_j} + mg\ \mathbf{r}_g^\times \mathbf{R}^{bl} \hat{\mathbf{k}} \right) \quad (2b)$$

where all quantities are measured in the body frame. We consider torques produced by momentum wheels, thrusters, and the gravity torque incurred by the offset of the payload's center of mass from the air bearing's center of rotation.

The parameter vector, $\mathbf{\Pi}$, does not enter into the kinematic ($\dot{\mathbf{q}}$) equation. Grouping the control torques, the dynamic ($\dot{\boldsymbol{\omega}}$) equation can be written such that it is clearly linear with respect to the parameters:

$$\mathbf{g}_{control} = \mathbf{I}_b \dot{\boldsymbol{\omega}} + \boldsymbol{\omega}^\times \mathbf{I}_b \boldsymbol{\omega} - mg \mathbf{r}_g^\times \mathbf{R}^{bi} \hat{\mathbf{k}} \quad (3a)$$

$$= [\dot{\boldsymbol{\omega}}] \{\mathbf{I}_b\} + [\boldsymbol{\omega}^2] \{\mathbf{I}_b\} - [\mathbf{q}^2] mg \mathbf{r}_g \quad (3b)$$

$$= \left[\left([\dot{\boldsymbol{\omega}}] + [\boldsymbol{\omega}^2] \right), [\mathbf{q}^2] \right] \mathbf{\Pi} \quad (3c)$$

Equation 3a is a trivial rearrangement of Equation 2b. In Equations 3b and 3c we manipulate terms in order to form matrices of the states multiplied by vectors of the parameters. Thus $[\dot{\boldsymbol{\omega}}]$ is a 3×6 matrix composed of elements that are functions of $\dot{\boldsymbol{\omega}}$, $[\boldsymbol{\omega}^2]$ is a 3×6 matrix filled with quadratic functions of $\boldsymbol{\omega}$, and $[\mathbf{q}]$ is a 3×3 matrix containing quadratic functions of the quaternions. The term $\{\mathbf{I}_b\}$ is a vector of the six unique elements in the moment of inertia matrix, and $mg \mathbf{r}_g$ completes the parameter vector $\mathbf{\Pi}$ with the components of the center-of-gravity vector as in Equation 1. It is clear from Equation 3b that the moments of inertia can be calculated given knowledge of the control torques, the angular velocities, and their derivatives. The mass and center of gravity are coupled and cannot be determined independently of one another; these terms are functions of the control torques and the attitude only.

A PRIORI ESTIMATES

We obtained initial estimates of the parameters through mass properties analysis of a CAD model. This model was of sufficient detail to include minor components and fasteners, but did not include the wiring harness. A crude model of the wiring was added in order to determine the magnitude of the error in the parameter initial conditions.

One way to confirm the validity of such a model is through a batch least squares technique. Such schemes have been used successfully for the air-bearing spacecraft simulators at Georgia Tech² and the Air Force Institute of Technology.^{3,4} More robust batch techniques were used for the University of Michigan's⁵ and the Naval Postgraduate School's⁶ systems. In each of these cases, agreement between the CAD model and the batch estimator was demonstrated to be within a reasonable error bound. However, the relationship of that error with respect to the physical system is unclear. As the DSACSS is intended to support a wide range of functions — from undergraduates in lab courses to graduate students' research projects — requiring that all controllers be sufficiently robust against rough approximations is impractical.

Proper application of a least squares method requires application of a control torque to provide a persistent excitation to the system. We have not yet performed such a data collection maneuver. Moreover, as we are interested in providing dynamic, real-time estimates of the parameters as they vary (for example, the change in the center-of-gravity vector as propellant is depleted with thruster firings) batch techniques appear limited in their usefulness.

CANDIDATE SEQUENTIAL FILTERS

The Extended Kalman Filter (EKF) is the most commonly used sequential filter for online estimation of spacecraft attitude dynamics. A first-order nonlinear filter, its optimality cannot (as in the case of the linear Kalman Filter⁷) be proven. However, the EKF is commonly successfully used to provide state estimates of continuous-time, nonlinear dynamic systems from noisy, discrete-time measurements. Attempts to address the first-order approximation shortcomings of the EKF — which can lead to instability of the filter — are not new.⁸⁻¹³

Estimation of spacecraft attitude via an EKF poses an additional challenge due to the numerical complexities associated with common attitude representations, *e.g.*, singularities associated with Euler angle representations or normalization of the quaternion. Work on mitigating these issues has been well documented; references cited here are provided only as a sampling of the literature.^{14–17}

More recent proposed improvements to the EKF have branched out into two areas of research. The two branches offer improved performance against different sources of error.¹⁸ One technique seeks to improve the convergence of the first-order filter by iterating at the measurement update step. These Iterated Extended Kalman Filters (IEKF) reduce the effective measurement noise. As such, they can be more tolerant to process noise and errors in initial conditions. Iterating in the measurement step also provides robustness against the first-order approximations of the derivatives.^{18,19}

The second family of modified nonlinear filters improve performance by eliminating the Jacobian representation of the derivatives. These filters can yield drastically improved behavior beyond the convergence of the EKF for the same order of floating point operations (flops). This class of filters, termed the Linear Regression Kalman Filters (LRKF), are beyond the scope of this paper but are included here for completeness.^{18,20–34} Some of these techniques have been further enhanced to capitalize on the improvements obtained through iteration in the IEKF and apply similar techniques to these higher-order filters.

The Unscented Kalman Filter (a member of the LRKF family) has recently been documented in its application to spacecraft attitude and orbital dynamics; such applications are unusual in a literature dominated by theory papers and neural network applications.^{35,36}

Filter Equations

Although we have not developed any new filtering equations in this work, some of the filters we are applying are uncommon in the field of spacecraft attitude dynamics and control or are being applied in new or atypical ways. A brief overview of the filter equations is included for completeness.

Extended Kalman Filter

The family of Kalman Filters can be developed in both continuous- and discrete-time forms. We make use of a hybrid set of equations that are continuous in the process and discrete in the measurement.

The time-update step for the continuous / discrete EKF is

$$\dot{\hat{\mathbf{x}}}(t) = \mathbf{f}(\hat{\mathbf{x}}(t), \mathbf{u}(t), \mathbf{\Pi}, t) \quad (4)$$

$$\dot{\mathbf{P}}(t) = \mathbf{F}(t)\mathbf{P}(t) + \mathbf{P}(t)\mathbf{F}(t)^\top + \mathbf{Q}(t) \quad (5)$$

$$\tilde{\mathbf{y}}_k = \mathbf{h}(\mathbf{x}_k) \quad (6)$$

where the first-order Jacobian approximation to the derivative of the process equation is

$$\mathbf{F}(t) \triangleq \left. \frac{\partial \mathbf{f}}{\partial \mathbf{x}} \right|_{\mathbf{x}(t)=\hat{\mathbf{x}}(t)} \quad (7)$$

and the model is initialized with the expected value of the initial state and its predicted error is

$$\hat{\mathbf{x}}(t_0) = \hat{\mathbf{x}}_0 \quad (8)$$

$$\mathbf{P}_0 = E\left\{(\mathbf{x}(t_0) - \hat{\mathbf{x}}_0)(\mathbf{x}(t_0) - \hat{\mathbf{x}}_0)^\times\right\} \quad (9)$$

The first order approximation to the ideal (linear) Kalman Gain is calculated by

$$\mathbf{K}_k = \mathbf{P}_k^- \mathbf{H}_k^{-\top} \left[\mathbf{H}_k^- \mathbf{P}_k^- \mathbf{H}_k^{-\top} + \mathbf{R}_k \right]^{-1} \quad (10)$$

where

$$\mathbf{H}_k^- \triangleq \left. \frac{\partial \mathbf{h}}{\partial \mathbf{x}} \right|_{\mathbf{x}_k = \hat{\mathbf{x}}_k^-} \quad (11)$$

The Kalman Gain is used in the measurement-update step for both the state vector and its covariance matrix as follows

$$\hat{\mathbf{x}}_k^+ = \hat{\mathbf{x}}_k^- + \mathbf{K}_k [\tilde{\mathbf{y}}_k - \mathbf{h}(\hat{\mathbf{x}}_k^-)] \quad (12)$$

$$\mathbf{P}_k^+ = [\mathbf{1} - \mathbf{K}_k \mathbf{H}_k^-] \mathbf{P}_k^- \quad (13)$$

Note that the innovations process, $\mathbf{z}_k = \tilde{\mathbf{y}}_k - \mathbf{h}(\hat{\mathbf{x}}_k^-)$, is evaluated at the time-update value of the state.

Iterated Extended Kalman Filter

The Iterated Extended Kalman Filter (IEKF) is initialized identically to the EKF; the time-update is also performed in the same way. The IEKF differs in the measurement-update step: the iterated filter updates the state and its covariance, then linearizes about this new point and cycles until the the measurement update of the state (Equation 16) converges to some value or exceeds a maximum number of iterations. That is, the innovations process for the IEKF is ultimately evaluated about the measurement-update value of the state. Equations 10–13 are modified to

$$\mathbf{K}_k = \mathbf{P}_k^- \mathbf{H}_k^{+\top} [\mathbf{H}_k^+ \mathbf{P}_k^- \mathbf{H}_k^{+\top} + \mathbf{R}_k]^{-1} \quad (14)$$

$$\mathbf{H}_k^+ \triangleq \left. \frac{\partial \mathbf{h}}{\partial \mathbf{x}} \right|_{\mathbf{x}_k = \hat{\mathbf{x}}_k^+} \quad (15)$$

$$\hat{\mathbf{x}}_k^+ = \hat{\mathbf{x}}_k^- + \mathbf{K}_k [\tilde{\mathbf{y}}_k - \mathbf{h}(\hat{\mathbf{x}}_k^+)] \quad (16)$$

$$\mathbf{P}_k^+ = [\mathbf{1} - \mathbf{K}_k \mathbf{H}_k^+] \mathbf{P}_k^- \quad (17)$$

Coupled Sequential Parameter Estimation

The simultaneous estimation of states and parameters is not a new problem. Techniques particularly applicable to spacecraft applications capitalize on the work done to couple attitude estimation.^{37,38} However, this work produced time-consuming, batch-estimation techniques not desirable for our application.

There are two simple extensions that can be applied to any Kalman Filter. These techniques — joint and dual filtering — use an analogous filter to estimate the parameters concurrently with the states. The joint method is the simpler of the two to conceptualize: the parameter vector of interest is simply appended onto the true state vector. The time-update for the latter portion of the augmented state vector allows no changes beyond the effects of process noise (*i.e.*, the parameters should be constant) but the entire augmented covariance matrix is propagated as one.^{19,20,39,40} The dual filtering technique intertwines a pair of distinct sequential filters, one estimating the true states and the other estimating the parameters.^{31,40–46}

Joint Filtering

The joint filter is initialized with

$$\hat{\mathbf{x}}_{aug}(t_0) = [\hat{\mathbf{x}}_0^\top, \hat{\mathbf{\Pi}}_0^\top]^\top \quad (18)$$

$$\mathbf{P}_{aug0} = E\left\{(\mathbf{x}_{aug}(t_0) - \hat{\mathbf{x}}_{aug0})(\mathbf{x}_{aug}(t_0) - \hat{\mathbf{x}}_{aug0})^\top\right\} \quad (19)$$

with a time update step of

$$\dot{\hat{\mathbf{x}}}_{aug}(t) = \begin{bmatrix} \mathbf{f}(\hat{\mathbf{x}}(t), \mathbf{u}(t), \hat{\boldsymbol{\Pi}}, t) \\ \mathbf{0} \end{bmatrix} \quad (20)$$

The actual filtering equations are as above.

Dual Filtering

The Dual Filtering equations are analogous to the state filtering equations. The time-update equations are the trivial (constant) case, provided here in discrete time form

$$\hat{\boldsymbol{\Pi}}_k^- = \hat{\boldsymbol{\Pi}}_{k-1}^+ \quad (21)$$

$$\mathbf{P}_{\boldsymbol{\Pi}_k}^- = \mathbf{P}_{\boldsymbol{\Pi}_{k-1}}^+ + \mathbf{Q}_{\boldsymbol{\Pi}_{k-1}} \quad (22)$$

There are several techniques for choosing the parameter process-noise matrix, $\mathbf{Q}_{\boldsymbol{\Pi}}$. We are using the “forgetting factor” technique, where

$$\mathbf{Q}_{\boldsymbol{\Pi}_k} \triangleq (\lambda^{-1} - 1)\mathbf{P}_{\boldsymbol{\Pi}_k}^+ \quad (23)$$

$$\mathbf{P}_{\boldsymbol{\Pi}_k}^- = \mathbf{P}_{\boldsymbol{\Pi}_{k-1}}^+ + (\lambda^{-1} - 1)\mathbf{P}_{\boldsymbol{\Pi}_k}^+ \quad (24)$$

$$= \lambda^{-1}\mathbf{P}_{\boldsymbol{\Pi}_{k-1}}^+ \quad (25)$$

The memory constant $\lambda \in (0, 1]$; λ is typically in the range from 0.997 – 0.999.⁴²

The Kalman Gain and associated measurement-update equations for the parameter EKF are

$$\mathbf{K}_{\boldsymbol{\Pi}_k} = \mathbf{P}_{\boldsymbol{\Pi}_k}^- \mathbf{E}_k^T \left[\mathbf{E}_k \mathbf{P}_{\boldsymbol{\Pi}_k}^- \mathbf{E}_k^T + \mathbf{R}_{\boldsymbol{\Pi}_k} \right]^{-1} \quad (26)$$

$$\hat{\boldsymbol{\Pi}}_k^+ = \hat{\boldsymbol{\Pi}}_k^- + \mathbf{K}_{\boldsymbol{\Pi}_k} \mathbf{e}_k \quad (27)$$

The innovations process of a dual filter can be conceptualized as the error in the equation of interest. To determine the parameters of an arbitrary system of equations, the error, \mathbf{e} , and its Jacobian matrix (with respect to the parameters, $\boldsymbol{\Pi}$), \mathbf{E} , are defined as

$$\mathbf{e}_k = \mathbf{d}_k - \mathbf{G}_k \quad (28)$$

$$\mathbf{E}_k = - \left. \frac{\partial \mathbf{e}}{\partial \boldsymbol{\Pi}} \right|_{\boldsymbol{\Pi}=\hat{\boldsymbol{\Pi}}_k^-} \quad (29)$$

To learn the parameters that dictate the state dynamics, $\mathbf{d}_k \rightarrow \dot{\hat{\mathbf{x}}}(t_k)$ and $\mathbf{G}_k \rightarrow \mathbf{f}(\hat{\mathbf{x}}_k, \hat{\boldsymbol{\Pi}}_k)$, yielding first-order approximate equations of

$$\mathbf{e}_k = \frac{\hat{\mathbf{x}}_k^+ - \hat{\mathbf{x}}_{k-1}^+}{t_k - t_{k-1}} - \mathbf{f}(\hat{\mathbf{x}}_k^+, \hat{\boldsymbol{\Pi}}_k^-) \quad (30)$$

$$\mathbf{E}_k = \left. \frac{\partial \mathbf{f}(\hat{\mathbf{x}}_k^+, \hat{\boldsymbol{\Pi}}_k^-)}{\partial \boldsymbol{\Pi}} \right|_{\boldsymbol{\Pi}=\hat{\boldsymbol{\Pi}}_k^-} \quad (31)$$

The measurement-update equations could be recast in terms of the IEKF framework by iterating to evaluate the error vector of Equation 30 and its Jacobian (Equation 31) with the updated parameters. We have not developed this technique in this paper.

SEQUENTIAL FILTER ANALYSIS

At the core of each of the DSACSS platforms is a PC/104+ form-factor computer. Each computer includes a 32-bit 133MHz Tri-M MZ104+ ZF×86 processor with 64MB of RAM. The operating system (a lean, customized version of Slackware Linux) and command software is stored on a 288MB

DiskOnChip solid-state memory device. Operational software is written in C++ with lower level software written in C for reasons of efficiency. Due to the relatively slow clock speed of the computers, computation time could become an operational constraint. As such, we do not want to load the processor with unnecessarily complex algorithms. We seek a balance between accuracy and computation time for effective state estimation.

Open Source Software Projects

The operational code and additional simulation tools for DSACSS laboratory work are maintained in a pair of open source software projects freely available for use. All DSACSS operational code, including filters and controllers, are contained in the DSACSS-Ops project. A diverse collection of simulation tools for both orbital and attitude dynamics are housed in an Open Source, Extensible Spacecraft Simulation and Modeling Environment Framework, Open-SESSAME.^{47,48} The purpose of these software projects is to provide a development framework both for simulation and operation that is easy to use, maintain, and expand upon.[§]

Simplified Equations of Motion

For the purposes of this investigation, we elected not to evaluate the full equations presented earlier. For simplicity and ease of analysis, we have restricted the area of interest of this study to the standard form of Euler’s rotational motion equation:

$$\dot{\mathbf{x}}(t) = \mathbf{I}_b^{-1} \left(-\mathbf{x}(t)^\times \mathbf{I}_b \mathbf{x}(t) \right) \quad (32)$$

where \mathbf{I}_b need not be diagonal. Considering only the measurements from the rate gyros yields a measurement equation of

$$\tilde{\mathbf{y}}_k = \mathbf{x}(t_k) \quad (33)$$

The Extended Kalman Filter requires evaluation of the process- and measurement-equation Jacobian matrices with respect to the states. For the case of full-state-feedback the measurement Jacobian is the identity matrix. The process Jacobian also reduces to a simple form but is worth some additional consideration, provided in the next section.

Evaluation of the Process Jacobian

For the purposes of this derivation we return to the full equations of motion presented in Equation 2. In this case,

$$\mathbf{F}(t) \triangleq \left. \frac{\partial \mathbf{f}}{\partial \mathbf{x}} \right|_{\mathbf{x}(t)=\hat{\mathbf{x}}(t)} \quad (34)$$

$$= \left[\begin{array}{c|c} \boldsymbol{\omega}^{4 \times} & \frac{1}{2} \mathbf{Q}(\mathbf{q}) \\ \hline mg \mathbf{r}_g^\times \frac{\partial \mathbf{R}^{bl} \hat{\mathbf{k}}}{\partial \mathbf{q}} & \mathbf{I}_b^{-1} \left(-\boldsymbol{\omega}^\times \mathbf{I}_b + (\mathbf{I}_b \boldsymbol{\omega})^\times \right) \end{array} \right] \quad (35)$$

where $\boldsymbol{\omega}^{4 \times}$ is a 4×4 skew-symmetric matrix of the angular velocities,

$$\boldsymbol{\omega}^{4 \times} \triangleq \left[\begin{array}{c|c} \boldsymbol{\omega}^\times & \boldsymbol{\omega} \\ \hline -\boldsymbol{\omega}^\top & 0 \end{array} \right] \quad (36)$$

the $\mathbf{Q}(\mathbf{q})$ matrix is as in the original process equation (2a), and

$$\frac{\partial \mathbf{R}^{bl} \hat{\mathbf{k}}}{\partial \mathbf{q}} = 2 \left[\begin{array}{cccc} q_3 & -q_4 & q_1 & -q_2 \\ q_4 & q_3 & q_2 & q_1 \\ -q_1 & -q_2 & q_3 & q_4 \end{array} \right] \quad (37)$$

[§]Please see <http://dsacss.sourceforge.net> and <http://spacecraft.sourceforge.net> for additional information on the open source software projects.

The complaint of having to compute the process Jacobian matrix at each timestep is twofold. Certainly it is computationally expensive. However, this closed-form solution provides a simple and precise means of performing the calculation. Moreover, noting the quadrant-wise definition allows us to make use of pre-calculated matrices already stored in memory. It should be noted that no amount of creative algebra will compensate for the first-order approximations of the derivatives in the standard EKF. This formulation will not effect the convergence of a filter for a highly nonlinear system.

For the simplified form of the equations used in this investigation only the lower right quadrant of the Jacobian matrix is applicable, thus

$$\mathbf{F}(t) = \mathbf{I}_b^{-1} \left(-\mathbf{x}(t)^\times \mathbf{I}_b + (\mathbf{I}_b \mathbf{x}(t))^\times \right) \quad (38)$$

RESULTS

We evaluate eight filters in this study. Baseline cases for both the EKF and the IEKF are evaluated with the true value of the parameters. Realistic cases for each are evaluated with the expected value of parameters — representative of the real-world case. Joint estimation schemes are run for both the EKF and the IEKF. We ran two dual state-parameter filters: an EKF-EKF and an IEKF-EKF. Values for both the true and expected moment of inertia matrices are shown in Table 1. Recall that the expected values were obtained from the nominal CAD model. The true values are based on an augmented CAD model, updated to include a simple model of the wiring harness.

Table 1: True and Expected Values of the Moment of Inertia Matrix

True			Expected		
6.5	-0.5	0.5	5.5	0.5	0.5
-0.5	5.5	0.0	0.5	5.5	0.5
0.5	0.0	10.5	0.5	0.5	9.5

Tuning

We begin this investigation by evaluating the behavior of the basic EKF and IEKF with variation of the process- and measurement-noise tuning parameters, $\mathbf{Q}(t)$ and \mathbf{R}_k . As indicated by the notation, these gains can be varied in time; we choose to hold them constant. Note that the process noise matrix is not constant in time for the parameter portion of the dual filters; see Equation 23 for explanation. The noise matrices are constrained to be diagonal. Because the system only includes one type of state and one type of sensor the diagonal terms are held consistent. That is, these matrices are entirely characterized by a single number. These constants are varied far beyond reasonable values in an attempt to get the filters to diverge.

Figures 2 and 3 show the behavior of the EKF and IEKF with variation of the noise matrices. Each plot displays the moving average of the l_2 norm (root-sum-square) of the state error. Development of this style of plot is discussed later.

Each plot shows the traces of five filters run with a wide range of process or measurement noise constants. The process noise constant is varied from 0 to a very large (10^{15}) value. The measurement noise constant is varied by adjusting the gyro error from 0 to 100 and choosing the constant to be the gyro standard deviation: the gyro error normalized by $\sqrt{2}$.

The filters running with the true values of the parameters converge regardless of the value of the

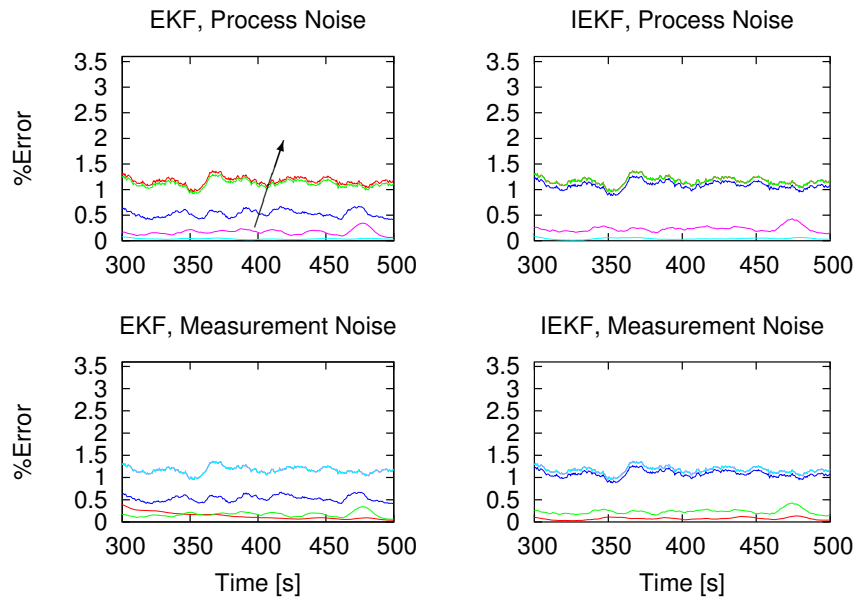


Figure 2: State % Error Root-Sum-Square Moving Average Behavior, True Parameters (arrow indicates direction of increasing noise, all subplots)

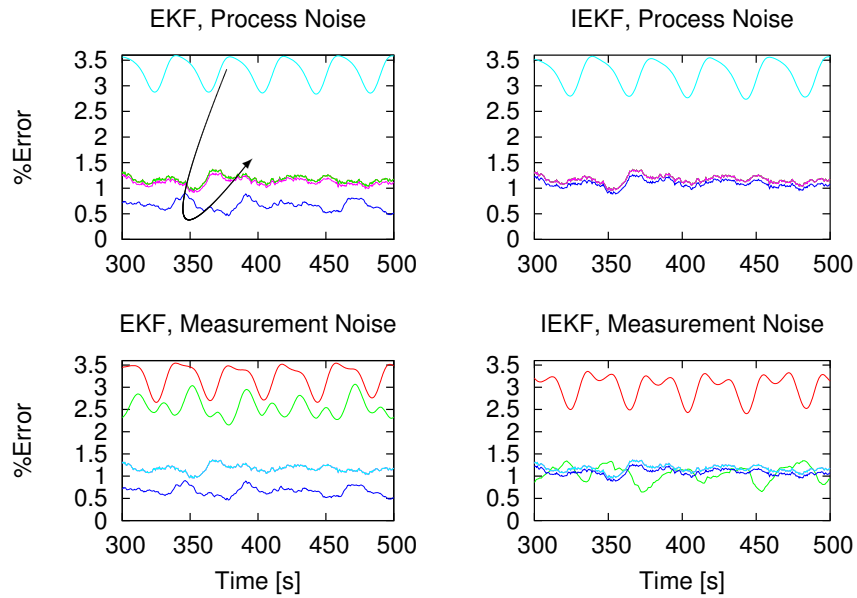


Figure 3: State % Error Root-Sum-Square Moving Average Behavior, Expected Parameters (arrow indicates direction of increasing noise, all subplots)

noise constants. Interestingly, the EKF calculates lower state errors for several sets of noise constants than the IEKF. However, the convergence of each of the filters displayed in Figure 2 is acceptable; note that this set of filters is initialized with the true value of the parameters, so such stability is to be expected.

The behavior of the converging filters in Figure 3, those with the real-world, expected value of the parameters, is identical to that of the corresponding true-parameter filters. An offset in the parameters effectively acts as process noise, thus those filters with unnaturally-low process noise constants diverged. Similarly, filters with high measurement noise constants were unable to compensate for the process error. The IEKF was more stable under variation of the measurement noise than the EKF; both were equally susceptible to process noise. Improved convergence of the IEKF despite poor representation of the measurement noise is reasonable as the IEKF mitigates the effect of sensor errors by iterating to nearly a $0 = 0$ case within which the value of the Kalman Gain matrix is largely irrelevant.

All subsequent filters are run with both the process noise and the gyro noise constants held at 0.1; all of the above filters converged with these values. However, the uniform behavior of these two groups of filters is indicative of a problem further illustrated in later tests: the difference between the true and expected values of the parameters is too small for this analysis to yield compelling results.

Convergence to State Vector

The measurements for the simulation are generated by propagating the exact equations of motion and adding Gaussian white random noise at a maximum amplitude of 10% of the state. As shown in Figure 4, the EKF initialized with the true parameter vector reduces this variation in noise appreciably. Figure 5 clarifies this improvement, indicating a filter noise band of 1.5%. All three states behave similarly. Initial convergence behavior of the filters is not shown; the different filter types display a variety of initial dynamics but this transient regime is of little importance in our application. All of the filters behave in a similar manner in the steady-state, thus these plots are not repeated for the other cases.

Convergence to Parameter Vector

One interesting conclusion of this work is that the joint filter for this set of equations is degenerate. Because the measurement equation provides direct feedback for the true state and no feedback into the parameters the joint filter is unable to vary the parameters. Regardless of the process noise assigned to the parameter terms the zeros of the measurement Jacobian matrix force the parameters to be held constant at their initial values.

The dual filters are successful in varying the parameters. The response of the parameters in the dual EKF-EKF is shown in Figure 6. The error in the parameters is presented as an absolute error in Figure 7. The dual filters are unable to overcome the bias dictated by the parameter initial conditions; the parameters typically vary by $\pm 0.5 \text{kg}\cdot\text{m}^2$. As noted above, future investigations should evaluate the performance of the dual filters with less-accurate expected values of the parameters.

Filter Performance Comparison

The raw error of the state and parameter vectors is prohibitively high-frequency for useful graphical comparison among filters. We have simplified their appearance by taking a moving average of the l_2 norm (root-sum-square) of the state- and parameter-error vectors (Figures 5 and 7, respectively). A 30-term moving average provides adequate smoothing with a reasonable loss of data quality for the state error. The most drastic loss of information caused by smoothing is an obvious representation of the maximum value of the errors: note that the state error consistently spikes to 1.5% in Figure 5

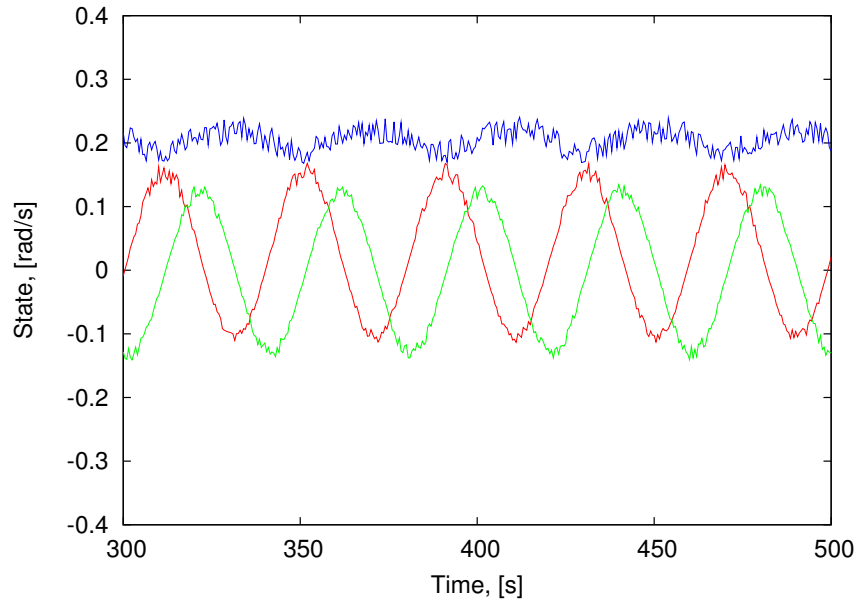


Figure 4: State Behavior for the Ideal EKF

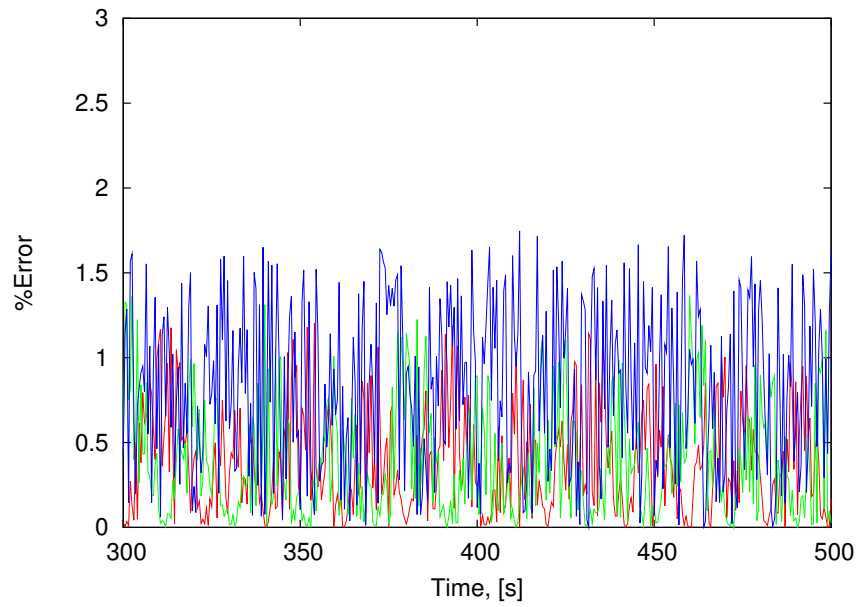


Figure 5: State Percent Error for the Ideal EKF

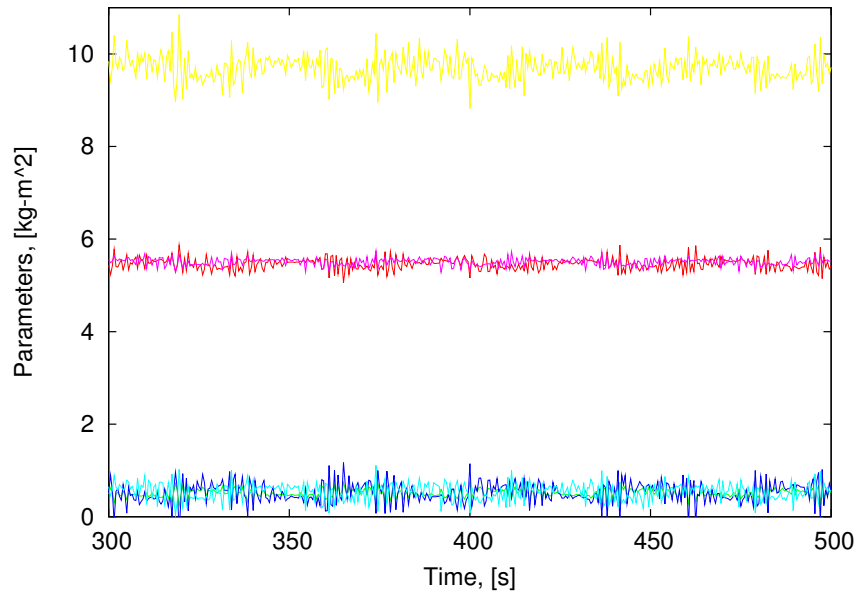


Figure 6: Parameter Behavior for the Dual EKF-EKF

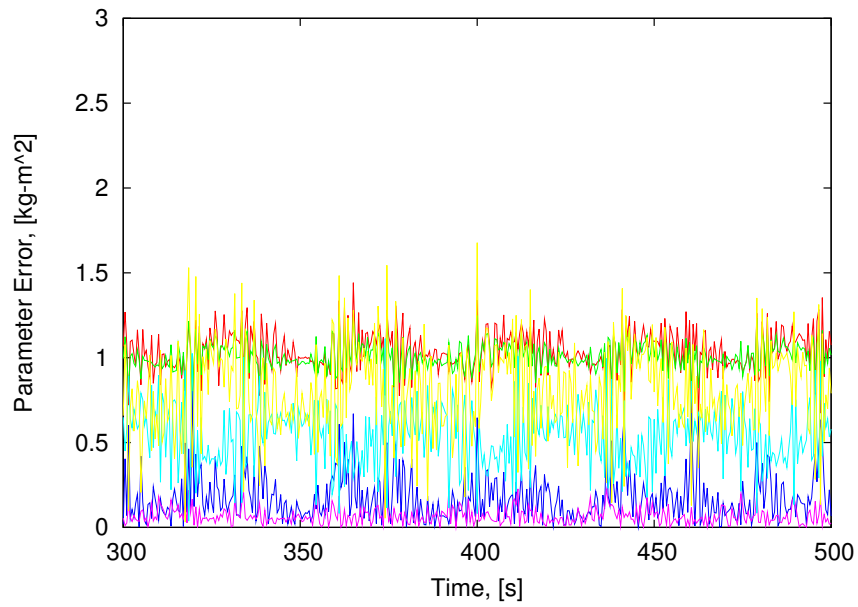


Figure 7: Parameter Absolute Error for the Dual EKF-EKF

while the smoothed line in Figure 8 remains below 1.25%.

Note that Figure 8 presents the state error root-sum-square moving average for all eight filters. However, only two distinct curves are visible, and these curves are only negligibly different. Specifically, the four EKF cases perform marginally better than the four IEKF cases regardless of parameter initial conditions or variation. Thus we can conclude that all of the filters perform to the same level of convergence for this set of noise constants. Moreover, all filters converge to a state error of less than 1.5%: for this simplified system, at least, parameter identification provided no additional performance. Again, greater variation in the parameters demands investigation.

As shown in Figure 9, the dual EKF-EKF and IEKF-EKF techniques yield different (but comparable) estimates for the parameters. The primary difference between the two curves is that the IEKF-EKF curve is substantially more erratic. These errors are smoothed with a moving average of 5 points; the persistently jagged nature of the smoothed IEKF-EKF curve indicates a much higher step-to-step variation of the estimates. Recall that in this dual filter the state is estimated with an IEKF while the parameters use an EKF. The IEKF typically yields a larger magnitude measurement update for the state, thus the error function for the dual filter is equivalently larger, resulting in greater parameter variation.

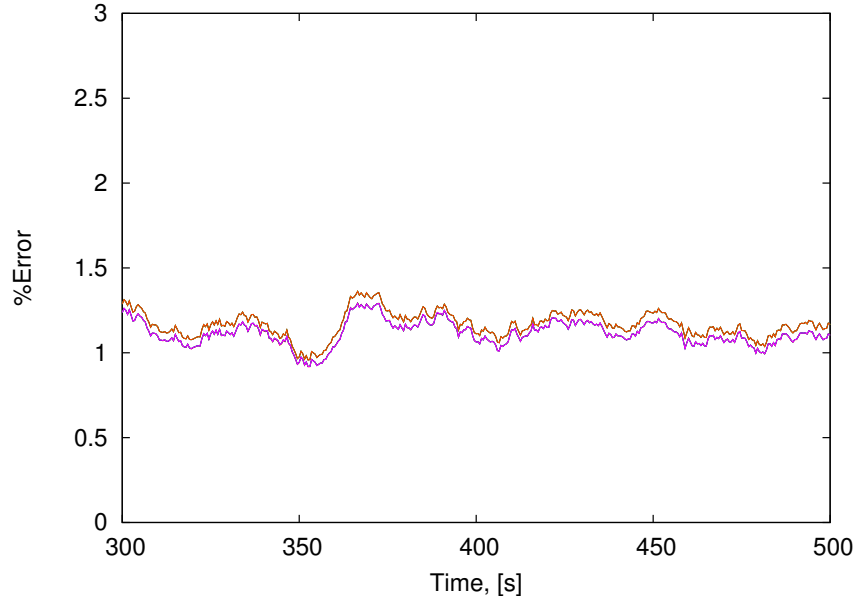


Figure 8: Moving Average for State Error, all filters

Given the filters' near-identical performance with respect to state calculation, the other available metric for comparison is filter computational time. This data is presented in Table 2. The IEKF converges to a tolerance of 10^{-3} within 10 iterations at each timestep. Most time steps required less than five iterations thus the IEKF did not require appreciably more computation time. Notably, the dual filters also required only an acceptably small increase in computation time. The joint filters, however, require a great deal of additional computation time; this is due to integrating the entire augmented state, an algorithm which could be substantially improved if warranted by estimation performance in future studies.

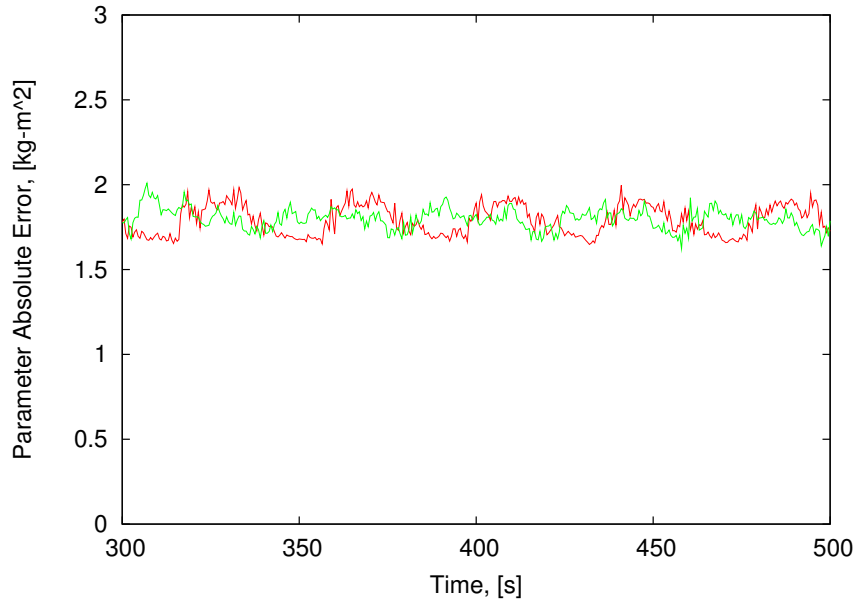


Figure 9: Moving Average for Parameter Error, Dual EKF-EKF and Dual IEKF-EKF

CONCLUSIONS

The intent of this work was to determine some subset of the filters under analysis for further evaluation with the complete equations of motion for the DSACSS platforms. However, the eight filters yielded such similar performance that any selections at this point would be premature. Some auxiliary conclusions can be made, however. We presented a closed-form solution of the state Jacobian matrix. Although this formulation does nothing to resolve the first-order approximation inherent in the derivation of the EKF, it is more accurate and computationally efficient than a finite different approximation. We have shown the joint filter is not numerically robust; it provided no variation of the parameters for our system. The EKF and IEKF demonstrated similar robustness under variation of the noise parameters. More detailed analysis of the behavior of these filters is required.

Table 2: Comparison of Run Times

Filter	Total Run Time [%]	Time Per Step [ms]
Ideal EKF	100%	42.15
Practical EKF	99.8%	42.08
Ideal IEKF	100.1%	42.20
Practical IEKF	99.1%	41.76
Joint EKF	124.2%	52.34
Dual EKF	106.9%	45.05
Joint IEKF	122.3%	51.55
Dual IEKF	109.8%	46.26

ACKNOWLEDGEMENTS

The authors are grateful to Matthew C. VanDyke of the Department of Aerospace & Ocean Engineering at Virginia Tech for many useful discussions regarding this problem.

REFERENCES

- [1] J. L. Schwartz, M. A. Peck, and C. D. Hall, “Historical Survey of Air-Bearing Spacecraft Simulators,” *Journal of Guidance, Control, and Dynamics*, vol. 26, pp. 513–522, July–August 2003.
- [2] B. Kim, E. Velenis, P. Kriengsiri, and P. Tsiotras, “A Spacecraft Simulator for Research and Education,” in *Proceedings of the AIAA/AAS Astrodynamics Specialists Conference*, no. 01-367, (Quebec City, Quebec, Canada), pp. 897–914, 2001.
- [3] G. S. Agnes and J. Fulton, “Design and Testing of SIMSAT — A Three-Axis Satellite Dynamics Simulator,” in *Proceedings of the 42nd AIAA/ASME/ASCE/AHS/ASC Structures, Structural Dynamics, and Materials Conference and Exhibit*, no. 01-1591, (Seattle, Washington), April 16–19, 2001.
- [4] R. Thurber, “Dynamic ground simulation of attitude control systems,” in *Proceedings of the 35th AIAA Aerospace Sciences Meeting & Exhibit*, no. 97-0010, (Reno, Nevada), January 6–9, 1997.
- [5] J. Ahmed, V. T. Coppola, and D. S. Bernstein, “Adaptive Asymptotic Tracking of Spacecraft Attitude Motion with Inertia Matrix Identification,” *Journal of Guidance, Control, and Dynamics*, vol. 21, September/October 1998.
- [6] M. G. Spencer, V. Chernesky, J. Baker, and M. Romano, “Bifocal Relay Mirror Experiments on the NPS Three Axis Spacecraft Simulator,” in *Proceedings of the AIAA Guidance, Navigation, and Control Conference and Exhibit*, no. 02-5031, (Monterey, California), August 5–8, 2002.
- [7] R. E. Kalman, “A New Approach to Linear Filtering and Prediction Problems,” *Transactions of the ASME—Journal of Basic Engineering, D*, vol. 82, pp. 35–45, 1960.
- [8] R. Kalman and R. Bucy, “New Results in Linear Filtering and Prediction Theory,” *Transactions of the ASME—Journal of Basic Engineering, D*, vol. 83, pp. 95–108, March 1961.
- [9] R. Bucy, “Nonlinear Filtering Theory,” *IEEE Transactions on Automatic Control*, vol. AC-10, p. 198, April 1965.
- [10] M. Athans, R. P. Wishner, and A. Bertolini, “Suboptimal State Estimation for Continuous-Time Nonlinear Systems from Discrete Noisy Measurements,” *IEEE Transactions on Automatic Control*, vol. 13, October 1968.
- [11] R. Bass, V. Norum, and L. Schwartz, “Optimal Multichannel Nonlinear Filtering,” *Journal of Mathematical Analysis and Applications*, vol. 16, pp. 152–164, 1966.
- [12] H. Kushner, “Dynamical Equations for Optimal Nonlinear Filtering,” *Journal of Differential Equations*, vol. 3, pp. 179–190, 1967.
- [13] H. Kushner, “Approximations to Optimal Non-Linear Filters,” in *Proceedings of the IEEE Joint Automatic Control Conference*, pp. 613–623, June 1967.
- [14] E. Lefferts, F. Markley, and M. Shuster, “Kalman Filtering for Spacecraft Estimation,” *Journal of Guidance*, vol. 5, pp. 417–427, September–October 1962.

- [15] M. D. Shuster, "Maximum Likelihood Estimation of Spacecraft Attitude," *Journal of the Astronautical Sciences*, vol. 37, pp. 79–88, January–March 1989.
- [16] M. D. Shuster, "A Simple Kalman Filter and Smoother for Spacecraft Attitude," *Journal of the Astronautical Sciences*, vol. 37, pp. 79–88, January–March 1989.
- [17] M. D. Shuster, "Kalman Filtering of Spacecraft Attitude and the QUEST Model," *Journal of the Astronautical Sciences*, vol. 38, pp. 377–393, July–September 1990.
- [18] T. Lefebvre, H. Bruyninckx, and J. D. Schutter, "Kalman Filters for Nonlinear Systems: A Comparison of Performance," Internal Report 01R033, Department of Mechanical Engineering, Katholieke Universiteit, Leuven, Belgium, October 2001. Submitted as Regular Paper to IEEE Transactions on Automatic Control, October 2001.
- [19] A. Gelb, ed., *Applied Optimal Estimation*. The M.I.T. Press, 1974.
- [20] J. L. Crassidis and J. L. Junkins, *Optimal Estimation of Dynamic Systems*. Boca Raton, Florida: CRC Press, to be published 2004.
- [21] S. J. Julier, J. K. Uhlmann, and H. F. Durrant-Whyte, "A New Approach for Filtering Nonlinear Systems," in *Proceedings of the American Control Conference*, vol. 3, pp. 1628–1632, June 21–23 1995.
- [22] S. J. Julier and J. K. Uhlmann, "A General Method for Approximating Nonlinear Transformations of Probability Distributions," tech. rep., Robotics Research Group, Department of Engineering Science, University of Oxford, 1994.
- [23] S. J. Julier and J. K. Uhlmann, "A New Extension of the Kalman Filter to Nonlinear Systems," in *Proceedings of the SPIE AeroSense International Symposium on Aerospace/Defense Sensing, Simulation and Controls*, (Orlando, Florida), April 20–25, 1997.
- [24] S. J. Julier and J. K. Uhlmann, "A Non-divergent Estimation Algorithm in the Presence of Unknown Correlations," in *Proceedings of the American Control Conference*, vol. 4, (Albuquerque, New Mexico), pp. 2369–2373, June 4–6, 1997.
- [25] S. J. Julier, "The Scaled Unscented Transformation," in *Proceedings of the American Control Conference*, vol. 6, pp. 4555–4559, 2002.
- [26] T. Lefebvre, H. Bruyninckx, and J. D. Schutter, "A Non-Minimal State Kalman Filter for Nonlinear Parameter Estimation Applied to Autonomous Compliant Motion," in *Proceedings of the IEEE International Conference on Robotics and Automation*, (Taipei, Taiwan), May 12–17, 2003.
- [27] M. Nørgaard, N. K. Poulsen, and O. Ravn, "Advances in Derivative-Free State Estimation for Nonlinear Systems," Tech. Rep. IMM-REP-1998-15, Technical University of Denmark, 2800 Lyngby, Denmark, April 7, 2000.
- [28] M. Nørgaard, N. K. Poulsen, and O. Ravn, "New Developments in State Estimation for Nonlinear Systems," *Automatica*, vol. 36, pp. 1627–1638, 2000.
- [29] T. S. Schei, "A Finite-Difference Method for Linearization in Nonlinear Estimation Algorithms," *Automatica*, vol. 33, no. 11, pp. 2053–2058, 1997.
- [30] E. A. Wan and R. van der Merwe, "The Unscented Kalman Filter for Nonlinear Estimation," in *Proceedings of the IEEE Symposium 2000: Adaptive Systems for Signal Processing, Communications, and Control*, (Lake Louise, Alberta, Canada), October 1–4, 2000.
- [31] E. A. Wan, R. van der Merwe, and A. T. Nelson, *Advances in Neural Information Processing Systems 12*, ch. Dual Estimation and the Unscented Transformation, pp. 666–672. MIT Press, 2000.

- [32] R. van der Merwe and E. A. Wan, “Efficient Derivative-Free Kalman Filters for Online Learning,” in *Proceedings of European Symposium on Artificial Neural Networks*, (Bruges, Belgium), April 2001.
- [33] E. A. Wan and R. van der Merwe, *Kalman Filtering and Neural Networks*, ch. 7, The Unscented Kalman Filter. Wiley, September 2001.
- [34] R. L. Bellaire, E. W. Kamen, and S. M. Zabin, “A New Nonlinear Iterated Filter with Applications to Target Tracking,” in *Proceedings of the International Society for Optical Engineering (SPIE) Conference on Signal and Data Processing of Small Targets*, vol. 2561, pp. 240–251, 1995.
- [35] D.-J. Lee and K. T. Alfriend, “Precise Real-Time Orbit Estimation Using the Unscented Kalman Filter,” in *Proceedings of the 13th AAS/AIAA Space Flight Mechanics Winter Meeting*, no. 03-230, (Ponce, Puerto Rico), February 9–13, 2003.
- [36] J. L. Crassidis and F. L. Markley, “Unscented Filtering for Spacecraft Attitude Estimation,” *Journal of Guidance, Control, and Dynamics*, vol. 26, July–August 2003.
- [37] F. L. Markley, “Attitude Determination and Parameter Estimation Using Vector Observations: Theory,” *Journal of the Astronautical Sciences*, vol. 37, pp. 41–58, January–March 1989.
- [38] F. L. Markley, “Attitude Determination and Parameter Estimation Using Vector Observations: Application,” *Journal of the Astronautical Sciences*, vol. 39, pp. 367–382, July–September 1991.
- [39] R. F. Stengel, *Optimal Control and Estimation*. Dover Publications, Inc., September 1994.
- [40] A. T. Nelson, *Nonlinear Estimation and Modeling of Noisy Time-Series by Dual Kalman Filtering Methods*. Doctor of Philosophy, Oregon Graduate Institute of Science and Technology, September 2000.
- [41] E. A. Wan and A. T. Nelson, *Kalman Filtering and Neural Networks*, ch. 5, Dual Extended Kalman Filter Methods. Wiley, September 2001.
- [42] S. Haykin, ed., *Kalman Filtering and Neural Networks*. John Wiley & Sons, Inc., 2001.
- [43] A. T. Nelson and E. A. Wan, “A Two-Observation Kalman Framework for Maximum-Likelihood Modelling of Noisy Time Series,” in *Proceedings of the IEEE International Joint Conference on Neural Networks*, pp. 2489–2494, 1998.
- [44] L. W. Nelson and E. Stear, “The Simultaneous On-Line Estimation of Parameters and States in Linear Systems,” *IEEE Transactions on Automatic Control*, vol. AC-21, no. 2, pp. 94–98, 1976.
- [45] E. A. Wan and A. T. Nelson, “Neural Dual Extended Kalman Filtering: Applications in Speech Enhancement and Monaural Blind Signal Separation,” in *Proceedings of the IEEE Workshop on Neural Networks for Signal Processing VII*, (Florida), September 1997.
- [46] E. A. Wan and A. T. Nelson, *Advances in Neural Information Processing Systems 9*, ch. Dual Kalman Filtering Methods for Nonlinear Prediction, Smoothing, and Estimation, pp. 793–799. MIT Press, 1997.
- [47] A. J. Turner and C. D. Hall, “An Open Source, Extensible Spacecraft Simulation and Modeling Environment Framework,” in *Proceedings of the AAS/AIAA Astrodynamics Specialist Conference*, no. 03-501, (Big Sky, Montana), August 3–7, 2003.
- [48] A. J. Turner, *An Open Source, Extensible Spacecraft Simulation and Modeling Environment Framework*. Masters of Science, Virginia Polytechnic Institute and State University, July 2003.